Substrate-Induced Modulation of Signal Transduction Networks

Citation: Jiang, P., A. C. Ventura, E. D. Sontag, S. D. Merajver, A. J. Ninfa, and D. Del Vecchio. "Load-Induced Modulation of Signal Transduction Networks." Science Signaling 4, no. 194 (October 11, 2011): ra67–ra67.

As Published: http://dx.doi.org/10.1126/scisignal.2002152

Publisher: American Association for the Advancement of Science (AAAS)

Persistent URL: http://hdl.handle.net/1721.1/86356

Version: Author's final manuscript: final author's manuscript post peer review, without publisher's formatting or copy editing

April 30, 2011

Substrate-induced modulation of signal transduction networks

P. Jiang[a], A. C. Ventura[b,d], E. D. Sontag[c], S. D. Merajver[d], A. J. Ninfa[a1], and D. Del Vecchio[e1]

[a]Department of Biological Chemistry, University of Michigan Medical School, Ann Arbor, MI; [b]Institute for Physiology, Molecular Biology, and Neuroscience, Department of Biology, University of Buenos Aires, Buenos Aires, Argentina; [c]Department of Mathematics, Rutgers University, New Brunswick, NJ; [d]Department of Internal Medicine, Comprehensive Cancer Center, University of Michigan, Ann Arbor, MI; [e]Department of Mechanical Engineering, Massachusetts Institute of Technology, Cambridge, MA

[1]correspondence: aninfa@umich.edu; ddv@mit.edu

Author contributions: P.J., A. C. V., S. D. M., A. J. N., D. D. V. designed research; P. J. performed experiments; D. D. V., A. C. V. performed theoretical analysis; E. D. S., S. D. M., A. J. N., D. D. V. analyzed results; A. J. N. , A. C. V., E.D.S., and D. D. V wrote the paper.

ABSTRACT

Biological signal transduction networks are commonly viewed as circuits that pass-along information -- in the process amplifying, enhancing sensitivity, or performing other signal-processing tasks -- to transcriptional and other components. Here, we report on a "reverse-causality" phenomenon, which we call substrate-induced modulation. Employing a combination of analytical and experimental tools, we discovered that signal communication is modulated, in a surprising way, by substrate components. Specifically, we found non-intuitive time-scale changes: for a first-order covalent modification cycle, the presence of substrates speeds-up signaling; by contrast, for a zeroth-order cycle, substrates slow-down signaling. The bandwidth, the range of frequency where the system can process information, decreases in the presence of substrates. This way, substrates participate in establishing trade-offs between noise-filtering capabilities and a circuit's ability to process high-frequency stimulation. We conclude that the view of signaling networks as independent relay devices, whose operating characteristics are not affected by their substrates, is fundamentally flawed. Our study highlights a fundamental and hereto unrecognized property of intracellular communication, bringing up issues that are generally relevant to biological signal transmission.

dynamics | modularity | signal transduction | substrates | regulatory networks

INTRODUCTION

A promising approach for unraveling the function of complex biological networks is to decompose them into functional modules [1-2] that have clearly defined functions, such as the sensing of extracellular ligands, signal transduction, gene expression, or metabolic control. The ultimate goal is to characterize the emergent collective function of networks from the knowledge of the behaviors of the individual modules, their interconnection topology, and character of their interactions.

In their fundamental review paper, Emonet et al. argued that the consideration of *system dynamics*, that is, time-dependent behavior, is a critical element in the process of delineating modules and determining their collective function [3]. Indeed, dynamics play a key role in function. For example, at the genetic level, transcriptional networks encode a variety of time-varying behaviors, such as the periodic changes of gene expression that are responsible for circadian rhythms and cell cycle timing [4-5]. Metabolic reaction pathways are regulated by environmental stimuli that vary over time [6]. The transient behavior of signaling systems controls gene activation patterns as well as diverse physiological processes ranging from bacterial chemotaxis, to cytoskeletal reorganization, to cell cycle checkpointing, to apoptosis [7-8]. Even when the steady state amount of an activated signaling protein lies within normal ranges, transient over-activation may result in aberrant signaling with severe consequences [9].

In this work, we perform a study of system dynamics and modularity, specifically focusing on signal transduction circuits. These circuits are commonly viewed as passing-along information to transcriptional and other components. In this classical view, the presence or absence of such components should not change the operating characteristics of the circuit. By contrast, recent theoretical work [10-13] has suggested that the behavior of discrete modules

might dramatically change upon coupling to other components through the effect of loads, just as in electrical, hydraulic, or mechanical networks. However, there has not been any experimental study of the dynamic effects of loads, nor have there been theoretical studies quantifying how the basic signal-processing time scales (response time, bandwidth) are affected. We report here on a striking "reverse-causality" phenomenon: employing a combination of analytical and experimental tools, we find that the time-scales of signal communication are modulated, in a surprising way, by the concentrations of substrate components. As a model system, we chose a ubiquitous motif in signal transduction, the covalent modification cycle. Experimentally, we used the reconstituted UTase/UR-PII cycle, which is derived from the nitrogen assimilation control network of *E. coli* [15]. This is a model system of highly purified components, which we can employ under conditions mimicking those found in *in vivo* signaling cascades such as the MAPK cascade. The covalent modification cycle is considered in two configurations: isolated, that is, without any substrate, and connected, that is, with its natural substrates, also called "loads". We analytically derive a novel extension of the standard Goldbeter-Koshland model for covalent modification [16] to include the effect of loads. Based on this mathematical model, analytical expressions for the response time and bandwidth as functions of the load and cycle parameters are obtained. We then employ the frequency response, a control theory tool, to determine how time-varying signals are transmitted. The basis of this approach is to measure the signaling system output in response to input signals oscillating at different frequencies [17]. Then, by comparing the frequency response and the step response of the isolated system to those of the connected system, one determines how downstream substrates control system dynamics.

We found that the response to time-varying input stimuli is dramatically altered by the presence of substrates, a phenomenon which we call *substrate-induced modulation* (SIM). When

the cycle enzymes operate in the saturated (zero-order) regime, SIM increases the response time. That is, the time required for the system to transition between the "on" and "off" states increases. By contrast, when the cycle enzymes operate in the unsaturated (first-order) regime, SIM leads to a decrease of the response time. The temporal profile of a stimulus determines how it is selectively transmitted through different cellular processes [18] and the quantity of information a pathway can carry depends on its bandwidth [19]. We found that SIM decreases system bandwidth, and that the extent of the decrease depends on whether one or both of the modified and unmodified forms of the cycle protein binds to substrates. The effect of SIM on bandwidth is more dramatic when only one of the two forms is bound, which is the circuit topology typically found in signaling networks. Finally, when only one form of the protein is bound by a downstream substrate, the dynamical effects of SIM are minimized by increasing the levels of the cycle enzymes. Conversely, when both modified and unmodified forms of the cycle protein are bound by substrates, the dynamical effects of SIM are minimized by reduction in the levels of the cycle enzymes.

The present work complements studies of stoichiometric retroactivity [20], that is, the effect of sequestering by downstream targets on the steady states of an upstream system. Related *in vivo* work using intact larvae also suggested that target effects may play a significant role in the distributions of components of MAPK cascades [21-22]. Stoichiometric retroactivity is a phenomenon different from SIM; indeed, it is known that even under conditions where the steady state behavior of a component is unaffected by substrates (no stoichiometric retroactivity), dynamic behavior may be dramatically altered [10-12]. Experimental evidence of this fact is also provided in this paper.

RESULTS

Mathematical Model Predictions

Fig 1A represents a general scheme of a covalent modification cycle with a downstream system to which it transmits information. Enzymes E_1 and E_2 catalyze the inter-conversion of the unmodified (W) and modified (W*) forms of the cycle protein, which bind to effective substrates λ and α, respectively. These substrates can represent proteins as in our experimental system, or another component that binds to the cycle protein, such as DNA. The input is a stimulatory effector (u) that regulates the enzyme activities and the output is the modified protein W*. A variety of regulatory patterns may be encountered; here, we assume that u is an absolute activator for E_2 and a non-competitive inhibitor for E_1 to match the experimental system (Fig 2A). Our results, however, do not depend on the mechanisms of the allosteric regulation. We refer to the system in Fig 1A as *isolated* when there are no substrates, while we refer to it as *connected* when the substrates are present. We extended the standard ordinary differential equation (ODE) model for covalent modification by Goldbeter and Koshland [16] to include the effect of substrates for either the unmodified or modified protein species. For a species X, we represent by X (italics) its concentration. In the experimental system, the quantity measured is the amount of the total modified protein, that is, $\overline{W} := W^* + \overline{C}$ (Fig 1A). The ordinary differential equation (ODE) describing the dynamics of $\overline{W}$ is given by (derived in *SI*):

$$\frac{d\overline{W}}{dt} = \frac{V_1}{(1+u/k'_D)} \frac{W_T - \overline{W}}{K_1(1+\lambda) + (W_T - \overline{W})} - V_2 \left(\frac{u}{\overline{k}'_D + u} \right) \frac{\overline{W}}{K_2(1+\alpha) + \overline{W}}$$

in which K_1 and K_2 are the Michaelis-Menten constants for the forward and backward modification reactions, respectively, W_T is the total amount of protein, $V_1 = k_1 E_{1T}, V_2 = k_2 E_{2T}$ are the maximal speeds of the forward and backward reactions, respectively (k_1, k_2 being the

catalytic rates and E_{1T}, E_{2T} being the total enzymes amounts), λ, α are the effective loads applied to W and W^*, respectively, u is the concentration of the stimulatory effector, and k_D' and $\bar{k}_D'$ are the dissociation constants of the stimulatory effector with enzymes E_1 and E_2, respectively. When $\alpha = 0$, the load is applied to W only. From the ODE, it is clear that the presence of the load increases the apparent Michaelis-Menten constants. We next study the consequence of this increase on the response time and bandwidth of the cycle.

SIM of rise and decay times. The rise and decay times quantify the time the cycle takes to switch steady state in response to a constant input stimulation. These times are of wide relevance for signaling systems and also for transcriptional networks, in which the turning on/off of a signaling pathway or of a gene has direct consequences on physiology [23]. The rise time is the time the output of the cycle $\overline{W}$ takes to rise from 10% to 90% of its overall excursion and the decay time is the time $\overline{W}$ takes to decay from 90% to 10% of its overall excursion. The results we obtain hold the same if we consider changes of the output between different percentages of the overall excursions, such as 5% and 95% or 1% and 99%. Here, we consider two cases: (a) when the cycle transitions between "on" ($\overline{W} = W_T$) and "off" ($\overline{W} = 0$) states in correspondence to extreme inputs *u=0* and *u* sufficiently large, respectively, to saturate the enzymes activities (*zero-order regime*); (b) when the cycle transitions between intermediate states in correspondence to non-extreme values of the input, so not to saturate enzyme activities (*first-order regime*).

(a) Zero-order regime. Analytical calculations of the rise and decay times employing our model (*SI*) gave the following expressions for the decay and rise times of the connected system:

$$t_{decay} = \frac{1}{V_2}\left(K_2(1+\alpha)\ln(9) + 0.8W_T\right) \qquad (1)$$

$$t_{rise} = \frac{1}{V_1}\left(K_1(1+\lambda)\ln(9) + 0.8W_T\right) \qquad (2)$$

which increase linearly with the amount of load. From these expressions, it follows that the system with load on both W ($\lambda > 0$) and W* ($\alpha > 0$) displays increased decay and rise times compared to the isolated system ($\alpha=\lambda = 0$). A system that has load applied only to W ($\lambda > 0$, but $\alpha = 0$) displays an increased rise time but the same decay time as the isolated system.

(b) First-order regime. Remarkably, when the input stimulation is intermediate so the enzymes operate in the first-order regime, SIM can result in faster responses (*SI*). Specifically, this occurs when the isolated system operates in the ultrasensitive regime ($K_1, K_2 << W_T$), and the load is sufficient to make the connected system operate in the hyperbolic regime ($K_1(1+\lambda), K_2(1+\alpha) >> W_T$), as in our experimental system [20]. Under these conditions, SIM makes responses faster when the input u is such that the corresponding maximal forward and reverse modification speeds $\frac{V_1}{(1+u/k_D')}, V_2\left(\frac{u}{\overline{k_D'}+u}\right)$ approach each other, causing the isolated system response to become slow (*SI*). SIM can have asymmetrical effects on the rise and decay times, causing one to increase while the other decreases. This occurs when, in addition to the above conditions, the forward and reverse reactions of the covalent modification cycle have different Michaelis-Menten constants or catalytic rates (*SI);* both of these conditions are obtained in our experimental system.

SIM of the bandwidth. The bandwidth of a system is the frequency band in which the system can process information. Here, we study how the same cycle can display different bandwidths depending on the specific configuration and amounts of its substrates. Let *A(ω)* be

the amplitude of the output response to periodic input stimuli of period $T=2\pi/\omega$. The bandwidth, denoted ω_B, is defined as the frequency at which $A(\omega)$ drops below $A(0)/\sqrt{2}$. A quantitative relationship between the bandwidth and the amounts of load can be determined by calculating the amplitude of response analytically from the model under the assumption of small amplitude sinusoidal input stimuli (about a bias level u_0) of the form $u(t) = u_0 + A_0 \sin(\omega t)$ (see *SI*). Even though sinusoidal inputs are not always biologically relevant, the system response to these inputs provides general information on the amplitude of response and bandwidth for more complicated input profiles. To complement the analysis based on sinusoidal inputs, we also considered input profiles in the form of a train of exponentially decaying pulses, which is closer to what we have in the experiments, and obtained the same qualitative results (*SI*). For the connected system, the bandwidth expression is proportional to the total amounts of enzymes E_{1T} and E_{2T}, to the catalytic rates k_1, k_2, and inversely proportional to the effective loads λ and α, for λ and α sufficiently large (see *SI* for the exact expressions). For large enough loads λ and α, the bandwidth of the connected system is lower than that of the isolated system, that is, $\omega_B{}^C < \omega_B{}^I$ (where "C" stands for "Connected" and "I" stands for "Isolated"). More generally, the expressions of the bandwidths depend on the amounts of load, on the isolated system operating regime (ultrasensitive or hyperbolic), and on the input amplitude (whether it is such that the enzymes operate in the zero-order or first-order regimes). Fig 1C,D,E illustrates the behavior of the bandwidth as a function of the Michaelis-Menten constants, the amounts of load, and the input amplitude. Sufficiently high amounts of load decrease the bandwidth of the connected system compared to that of the isolated system. However, for a fixed amount of load, decreasing the input amplitude, i.e., making the enzymes operate in the first-order regime, decreases also the difference between the isolated and connected systems bandwidths. If the input amplitude can be

set to sufficiently low values and the isolated system operates in the ultrasensitive regime (K_1, $K_2 << W_T$), small amounts of load can theoretically increase system bandwidth (Fig 1C). Finally, in the system with single load the decrease of bandwidth is more dramatic compared to the case in which $\lambda=\alpha>0$ (*SI*). These results are summarized in Fig 1B.

Insulation from SIM varying enzyme amounts. To explore the effect of changing the enzyme amounts on SIM, we computed the relative error $\Delta = \frac{A^I(\omega) - A^C(\omega)}{A^I(\omega)}$ between the amplitudes of the connected and isolated system responses (*SI*). The effect of changing the amounts of enzyme depends on whether the isolated system operates in the ultrasensitive or hyperbolic regime. Specifically, if the isolated system operates in the ultrasensitive regime, decreasing the amounts of enzymes makes the amplitudes of the isolated and connected systems approach each other. By contrast, if the isolated system operates in the hyperbolic regime, decreasing the amounts of enzymes makes the amplitudes of the isolated and connected systems become far apart from each other. Finally, when the load is applied to one side only, for inputs operating at sufficiently low values (the input bias u_0 is sufficiently small), decreasing the amounts of enzymes makes the amplitudes of the isolated and connected systems become further apart from each other. These results are summarized in Fig 1B, in which we have denoted $V=V_1$ and $V_2=aV_1$, for some positive constant a, and W_0 is the equilibrium value corresponding to the bias input u_0. In summary, if the isolated system operates in the ultrasensitive regime, an effective mechanism to attain dynamic insulation from substrates is to decrease the amount of the cycle enzymes; if the isolated system operates in hyperbolic regime or the load is applied to one side only, increasing the amounts of enzymes is an effective mechanism to attain insulation.

Experimental Results

The model system employed in the experiments is a reconstituted UTase/UR-PII covalent modification cycle of *E. coli* (Fig 2A) [15]. The bifunctional Uridylyltransferase/Uridylyl-Removing (UTase/UR) enzyme catalyzes the uridylylation of the PII protein via its UT activity and catalyzes the de-uridylylation of PII-UMP via its UR activity. These reactions are regulated by glutamine, an allosteric effector that binds to a sensory domain on the UTase/UR to inhibit the UT activity and activate the UR activity. Reactions are also regulated by α-ketoglutarate and adenylate energy charge, which directly control PII [24, 25]. Our experiments are performed at a fixed α-ketoglutarate and at high ATP/ADP ratio so that the system responds to glutamine as its sole stimulatory effector, producing uridylylation response to changes in glutamine similar to that of any covalent modification system including phosphorylation [20]. PII and PII-UMP interact with various downstream receptors involved in nitrogen assimilation [26]. Here, we study the effect of one PII receptor, the NRII protein of *E. coli* [15], on the transient response of the UTase/UR-PII cycle to time-varying concentrations of glutamine. For this experimental system to provide general results relevant for *in vivo* covalent modification cycles, we choose concentrations of proteins and enzymes in accordance to what is found in MAPK cascades [27]. In particular, the downstream substrate of the MAPKKK is found in amounts about two orders of magnitudes larger than the amounts of MAPKKK. Hence, we choose amounts of the NRII about 10 times larger than those of the upstream PII protein. If discernible effects of NRII will be detected in these conditions, then they will also be detected for higher NRII concentrations. Similarly, the amounts of converting enzymes of the MAPKKK cycle are about an order of magnitude smaller than the amounts of MAPKKK. Hence, we choose amounts of UTase enzyme varying from the same order as to two orders of magnitude smaller than the amounts of PII.

The PII protein is a trimer, and thus its uridylylation state can vary from zero to three modifications per trimer (Fig 2B). Hence, comparing Fig 1A with Fig 2A and Fig 2B, we have that W is unmodified PII (P_0 of Fig 2B) while the modified protein W* comprises all of the modified forms of PII (P_1, P_2, and P_3 of Fig 2B). In order to study also a circuit configuration where the load is applied to only one form of the protein (Fig 2C), a mutated system has been developed [20] consisting of a population of PII trimers, mostly heterotrimers, in which one of the three subunits is wild-type and two of the three subunits contain a small alteration that prevents their interaction with NRII or UTase/UR (Fig 2D). This heterotrimeric form of PII, which we refer to as "monovalent PII", is uridylylated and de-uridylylated normally by the UTase/UR in response to glutamine; NRII can bind to de-uridylylated PII but not to uridylylated PII [20].

SIM of rise and decay times. *(a) Zero-order regime.* To examine the rise time, the UTase/UR and PII were incubated with all necessary reaction components save UTP (which contained α-^{32}P-UTP to allow measurement of uridylylation), and at time zero in the experiment, UTP was added. To examine the decay time, the intact system, including UTP, was incubated in the absence of glutamine for sufficient time to allow it to reach the steady state corresponding to almost complete uridylylation, after which glutamine was added to the saturating concentration of 10 mM. These experiments were performed for both the isolated (without NRII) and connected (with NRII) systems, for systems with wild type PII (Fig 2A,B) and monovalent PII (Fig 2 C,D). NRII had a dramatic effect on both the rise time (Fig 3A) and decay time (Fig 3B) for the system containing wild type PII (system with double load, corresponding to Fig 2A); it increased both decay and rise times as expected from equations (1,2). Note that in Fig 3A SIM only altered the transient response, while the final steady state is not affected. When monovalent

PII was employed (system with single load, corresponding to Fig 2C,D), NRII caused a dramatic increase of the rise time (Fig 3C), but did not affect the decay time (Fig 3D), as expected from equations (1,2) with $\alpha=0$. With the level of NRII used in our experiments, the decay time doubled and the rise time increased by a factor of 4.75 in the wild type PII system. In the system with monovalent PII, the rise time was increased by a factor larger than 4.

(a) First-order regime. To measure the decay time upon intermediate stimulation, systems with wild-type PII (+/- NRII) were allowed to evolve in the absence of glutamine until the steady state had been obtained (corresponding to high uridylylation), after which glutamine was added to intermediate values (0.5 mM, 0.8 mM, 1.5 mM). At 0.8 mM glutamine, the connected system clearly displayed a decreased response time relative to the isolated system (Fig 3E); that is, consistent with our theoretical analysis SIM made the response faster. In the parallel experiments where glutamine was at 0.5 mM, no significant difference between the decay times of isolated and connected systems could be discerned, as expected (*SI*). When glutamine was at 1.5 mM, it also appeared that the connected system was faster than the isolated system, but the difference appeared to be smaller than when glutamine was at 0.8 mM (*SI*). To measure the rise time upon intermediate stimulation, various concentrations of glutamine (0.5 mM, 0.8 mM, 1.5 mM) were included in the reaction mixtures from the outset. Under these conditions, the steady-state uridylylation level corresponds to a lower concentration of uridylylated subunits than that obtained in the absence of glutamine. We were not able to identify conditions under which the rise time of the connected system was faster than the isolated system, although we observed that the difference between the connected and isolated systems became smaller as the glutamine concentration was increased. We also examined the rise time of the system containing monovalent PII, in the presence of intermediate glutamine concentrations (0.4 mM, 0.6 mM);

under both of these conditions, the difference between connected and isolated systems was larger than was the case at zero glutamine. Thus, in our experimental systems, SIM had asymmetrical effects at intermediate stimulation; it decreased the decay time but increased the rise time.

SIM of the bandwidth. Experimentally determining system bandwidth requires a method for imposing a time-varying input stimulation on the system. In our experimental system, the stimulatory effector is the amino acid glutamine. To remove glutamine from the system, we included a purified glutaminase (pyridoxal phosphate synthase from *Geobacillus stearothermophilus*). Periodic injection of glutamine in the presence of the glutaminase resulted in a sharp rise in the glutamine concentration upon injection, followed by an exponential decay of the glutamine concentration, similar to the output that may result from a relaxation-type oscillator. We varied the rate of decay of glutamine and amplitude of the response to glutamine injection by altering the concentration of the glutaminase in the system; we varied the amplitude of the input stimulation simply by injecting more glutamine (*SI*, Figure 10). The frequency of stimulation was controlled simply by injecting glutamine at the desired intervals. The response of the reconstituted UTase/UR-PII monocycle to periodic changes in glutamine concentration in the presence or absence of NRII is shown in Fig 4; amplitudes were estimated as described in the *SI*. NRII had a dramatic effect on the amplitude of response and bandwidth of the system for both the wild type UTase/UR-PII cycle (Fig4A,D) and the cycle with monovalent PII (Fig 4E,H). In both cases, the presence of NRII caused a decrease of the amplitude of response and of the bandwidth (Fig 4 D, Fig 4H). In particular, with wild-type PII a 13.2 % decrease in bandwidth was caused by NRII. (Fig 4D). With monovalent PII, the decrease of bandwidth was more dramatic as it decreased of 21% (Fig 4H). For both systems, we could identify a suitable input frequency where the isolated system demonstrated a significant response, while the connected

system essentially failed to respond (Fig 4C, Fig 4G). Thus, the presence of substrates decreased the bandwidth of the covalent modification cycle and the amplitude of response. There are some additional features to note about the plots of Fig 4. When the frequency of the input stimulation increases, the peaks of the response tended to monotonically decrease. This is due in part to the transient response of the system, which has not yet extinguished in the duration of the experiment. Also, when the input frequency becomes very high (Fig 4 C, Fig 4G), glutamine is not completely removed by the glutaminase and accumulates so that eventually the trajectories saturate to their low values (*SI*). Finally, slow decay in the rate of the glutaminase activity during the course of the experiments leads to a slight widening of each peak as the experiments progress.

Theory predicted that for a fixed amount of load, decreasing input amplitude would decrease the difference between the isolated and connected system bandwidths. In order to study this, we performed experiments where a lower amount of glutamine was added with each injection. Fig 5 shows the responses to inputs at different injection frequencies, in which the level of glutamine was increased by 1.5 mM with each addition (as opposed to 5 mM in Fig 4). This concentration is well within the range that the system can sense, and a low concentration of glutaminase was used in the experiments, such that the rate of decay of glutamine was reduced compared to the experiments of Fig 4. As shown in Fig 5, amplitudes of both isolated and connected systems fell as frequency was increased, but much less dramatically than in Fig 4A,D. Most importantly, we could not find a frequency at which the isolated system responded and the connected system did not (compare Fig 4C, where the injections were every 22 min with Fig 5B, where the injections were every 18 min). Indeed, the re-plot in Fig 5D shows that the bandwidths of the isolated and connected systems were very close to each other, confirming the theoretical predictions. In our

experiments, there is a limit to the frequency at which one can add glutamine, which is related to the level of glutamine added and the decay rate (glutaminase level). When the decay rate is very slow and the frequency of addition is high, glutamine will not be completely degraded after each pulse and will build up in the system. This seems to be the case in Fig 5C.

Insulation from SIM by varying enzymes amounts. Experiments similar to those in Fig 4 were performed with different amounts of the UTase enzyme. This is shown in Fig 6 for systems with wild type PII (Fig 6 A,D) and monovalent PII (Fig 6 E,G), with the re-plots of the amplitudes as a function of the enzyme amounts (Fig 6D, 6G) including data from Fig 4 with the same stimulation frequency at high enzyme concentration. In the system with wild-type PII, decreasing the enzyme amounts decreased the difference between the output amplitudes of the isolated and connected systems. The opposite pattern was observed when the system with monovalent PII was examined; increasing the amounts of enzyme made the amplitudes of the connected and isolated systems closer to each other (Fig 6G). This confirms our theoretical predictions (Fig 2B).

DISCUSSION

We have illustrated through theory and experiments how SIM affects the dynamics of a covalent modification cycle, a common component of signaling networks. Specifically, SIM controls the defining characteristics of dynamic behavior, response time and bandwidth, in non-intuitive ways. Our methodology is based on comparing the step and frequency responses of a signaling component in isolation to the same responses when the signaling component is connected to its substrates. This way, we can precisely capture the interaction between individual network modules and determine the emergent network behavior. The experimental system is an

in vitro reconstituted covalent modification cycle of *E. coli*, which is employed under conditions (amounts of proteins, enzymes, and targets) that mimic what is found in *in vivo* signaling cascades, such as the MAPK cascade. Hence, the effects found in this paper are expected to have significant physiological impact in concrete *in vivo* systems.

The frequency response determines a system's ability to respond to high-amplitude and low frequency signals that are physiologically significant, while filtering out high-frequency, low amplitude input signals that are not physiologically significant (noise) [14]. SIM can dramatically reduce the bandwidth of the system, such that the system filters out signals that it would be able to respond to in the absence of substrates (Fig 4C and Fig 4G). Since SIM can quench responses to time-varying stimulation, it may be employed to develop small-molecules as therapeutic substrates that diminish aberrant signaling occurring in various disease states [9].

Evolution or human engineering of complex signaling networks may be facilitated by conditions minimizing SIM as SIM minimization guarantees modular behavior. We showed that the amounts of the converting enzymes in a signaling system control the extent of the dynamic effects of substrates and that dynamic insulation from substrates may be obtained by suitably changing the amounts of cycle enzymes. Hence, our finding suggests a possible mechanism for attaining insulation from substrates and hence for engineering insulation devices in synthetic biology [10,28]. In many cellular signaling systems, downstream substrates bind to just one of the cycle proteins and converting enzymes are typically found at high or comparable concentrations relative to their substrate proteins. Our results hence suggest evolutionary pressure in signaling systems to serve as insulation devices to enforce unidirectional signal propagation, which is essential in any signal transmission device.

In summary, the view of signaling networks as independent relay devices, with operating characteristics that are not affected by their substrates, is misleading. Our study identified a fundamental and hereto unrecognized property of intracellular communication. Structural modules are not dynamically insulated from each other as interconnection to substrates changes individual dynamic behavior in non-intuitive ways. These issues are generally relevant to biological signal transmission and have direct repercussions on emergent network behavior and, ultimately, on physiology.

MATERIALS AND METHODS

Purified proteins. PII, UTase/UR and NRII proteins were prepared as described previously [20]. Heterotrimeric monovalent PII was prepared as described before [24]. Briefly, we formed heterotrimeric PII by gently dissociating the subunits of wild-type and Δ47-53 mutant PII, mixing at a ratio of 6 mutant subunits per wild-type subunit, and then allowed the subunits to re-associate. Under these conditions, the vast majority of wild-type subunits become incorporated into trimers with two mutant subunits. We were greatly assisted by Amber Smith of the Janet Smith Laboratory (Life Sciences Institute, University of Michigan) in the indentification and purification of a suitable glutaminase enzyme. She suggested the pyridoxal phosphate synthase from the thermophile *Geobacillus stearothermophilus,* provided us with the expression plasmids for this enzyme, and suggested purification methods [29]. This glutaminase has a low *Km*, of ~ 0.5 mM glutamine, can be produced at high concentration, has suitable activity, and apparently does not interfere with our reconstituted systems. In the *SI*, we show how glutaminase can be used to create time-varying input signals.

UTase/UR-PII monocycle dynamic experiments. The reaction mixture contained 100 mM Tris-Cl, pH 7.5, 10 mM $MgCl_2$, 100mM KCl, 0.3 mg/ml BSA, 0.2 mM α-ketoglutarate, 1mM ATP, 2 mM α-[^{32}P]-UTP or as indicated, 3 μM PII (homotrimers), UTase/UR as indicated, NRII as indicated, PLPS (24-meric complex, concentration stated as the concentration of each of the two types of subunits) as indicated. The reactions were performed at 30 ^{o}C and were initiated by addition of a mixture of the nucleotides (UTP and ATP). After incubated for 10 to 30 minutes, glutamine was added to 5mM (or as indicated). Aliquots were taken at time intervals and spotted onto P81 cellulose-phosphate filters (Whatman) and washed extensively in 5% TCA. The levels of incorporation of radioactive label into PII were quantified by liquid scintillation counting. For dynamic experiments with monovalent PII, the reaction conditions and procedure were the same except wild-type PII was substituted by 2 μM heterotrimeric PII mixture, which was formed from a six-fold excess of (Δ 47-53) subunits over wild-type subunits, as before [20].

REFERENCES

1 Alon U (2003) Biological networks: the tinkerer as an engineer. *Science* **301:**1866–1867.

2 Hartwell LH, Hopfield JJ, Leibler S, Murray AW (1999) From molecular to modular cell biology. *Nature* **402:**47–52.

3 Emonet T, Alexander RP, Kim PM, Gerstein MKB. (2009) Understanding modularity in molecular networks requires dynamics. *Science Signaling* **2:**1–4.

4 Dunlap J (1999) The molecular bases for circadian clocks. *Cell* **96:** 271–290.

5 Laub MT, McAdams HH, Feldblyum T, Fraser CM, and Shapiro L. (2000) Global analysis of the genetic network controlling a bacterial cell cycle. *Science* **290:**2144–2148.

6 Nishikawa T, Gulbahce N, Motter AE (2008) Spontaneous reaction silencing in metabolic optimization. *Plos Computational Biology* 4, e1000236.

7 Marshall CJ (1995) Specificity of receptor tyrosine kinase signaling: transient versus sustained extracellular signal-regulated kinase activation. *Cell* 80:179-185.

8 Hoffmann A, Levchenko A, Scott ML, Baltimore D (2002). The ikappaB-nf-kappaB signaling module: temporal control and selective gene activation. *Science* 298:1241-1245.

9 Blume-Jensen P, Hunter T (2001). Oncogenic kinase signalling. *Nature* **411:**355-365.

10 Del Vecchio D, Ninfa AJ, Sontag ED (2008) Modular cell biology: Retroactivity and insulation. *Mol. Syst. Biol* 4:161.

11 Ventura AC, Sepulchre J-A, Merajver SD (2008) A hidden feedback in signaling cascades is revealed. *PLoS Comput Biol* **4:**e1000041.

12 Saez-Rodriguez J, Kremling A, Gilles E (2005) Dissecting the puzzle of life: modularization of signal transduction networks. Comput Chem Eng 29: 619–629.

13 Sauro HM, Kholodenko BN (2004) Quantitative analysis of signaling networks. Prog Biophys Mol Biol 86: 5–43

14 Gomez-Uribe C, Verghese GC, Mirny LA (2007). Operating regimes of signaling cycles: statics, dynamics, and noise filtering. *PLoS Comp. Biol.* 3: e246.

15 Ninfa AJ, Jiang P, Atkinson MR, Peliska JA (2000) Integration of antagonistic signals in the regulation of nitrogen assimilation in *Escherichia coli*. *Current Topics Cell. Regul.* **36:**31–75.

16 Goldbeter A, Koshland DE (1981) An amplified sensitivity arising from covalent modification in biological systems. *Proc. Natl. Acad. Sci. USA* **78:**6840–6844.

17 Mettetal JT, Muzzey D, Gomez-Uribe C, van Oudenaarden A (2008) The frequency dependence of osmo-adaptation in *Saccharomyces cerevisiae*. *Science* **319:**482-484.

18 Behar M, Dohlman HG, Elston TC (2007) Kinetic insulation as an effective mechanism

for achieving pathway specificity in intracellular signaling networks. *Proc. Natl. Acad. Sci. USA*, **104:**16147–16151.

19 Hersen P, McClean MN, Mahadevan L, Ramanathan S (2008) Signal processing by the HOG MAP kinase pathway. *Proc. Natl. Acad. Sci. USA* **105:**7165–7170.

20 Ventura AC, Jiang P, VanWassenhove L, Del Vecchio D, Merajver SD, Ninfa AJ (2010). Signaling properties of a covalent modification cycle are altered by a downstream target. *Proc. Natl. Acad. Sci. USA* **107:** 10032-10037.

21 Kim Y, Coppey M, Grossman R, Ajuria L, Jimenez G, Paroush Z, Shvartzman SY (2010) MAPK substrate competition integrates pattern signals in the *Drosophila* embryo. *Current Biol* 20, 446-451.

22 Kim, Y., Paroush Z, Nairz K, Hafen E, Jim´enez G, and Shvartsman SY (2011) Substrate-dependent control of MAPK phosphorylation *in vivo*. *Mol. Sys. Biol.* 7:467.

23 Khodolenko BN, Hancock JF, Kolch W (2010) Signalling Ballet in Space and Time. *Nature Rev Mol Cell Biol.* **11:**414-426.

24 Jiang P, Ninfa AJ (2009) Sensation and signaling of alpha-ketoglutarate and adenylylate energy charge by the Escherichia coli PII signal transduction protein require cooperation of the three ligand-binding sites within the PII trimer. *Biochemistry* **48:**11522-11531.

25 Jiang P, Ninfa AJ (2007). *Escherichia coli* PII signal transduction protein controlling nitrogen assimilation acts as a sensor of adenylylate energy charge *in vitro*. *Biochemistry*, **46:**12979–12996.

26 Ninfa AJ, Jiang P (2005) PII signal transduction proteins: sensors of α-ketoglutarate that regulate nitrogen metabolism. *Curr Opinion Microbiol* **8:**168–173.

27 Huang, C. F., and J. E. Ferrell (1996). Ultrasensitivity in the mitogen-activated proteinkinase cascade. *Proc. Natl. Acad. Sci. USA* 93:10078–10083.

28 Jayanthi S, Del Vecchio D (2010) Retroactivity Attenuation in Bio-molecular Systems Based on Timescale Separation. *IEEE Trans. Aut. Control* (in press).

29 Zhu J, Burgner JW, Harms E, Belitsky BR, Smith JL (2005). A new arrangement of (beta/alpha)$_8$ barrels in the synthase subunit of PLP synthase. *J. Biol. Chem.* **280:** 27914-27923

Figure Legends

Figure 1. SIM of the bandwidth (analytical model results). A. General depiction of a covalent modification cycle. E_1 and E_2 represent the converter enzymes of the cycle, which are allosterically controlled by stimulatory effector u. The cycle protein W is inter-converted to a modified form W*. α and λ represent the effective load applied to W* and W, respectively, forming complexes $\overline{C}$ and C, respectively. The input u is a periodic signal with frequency ω and with amplitude A_0. **B.** Table summarizing the effect of SIM on the bandwidth. Here, ω_B denotes the bandwidth of the cycle, the superscripts denote "connected" (C) and "isolated" (I), and V is proportional to the amounts of enzymes. **C,D,E.** Behavior of the bandwidth as a function of the effective load, the input amplitude, and the cycle operating regime. The isolated system corresponds to the "0" point on the horizontal axis. When the isolated system steady state response is hyperbolic (**E**), the bandwidth monotonically decreases with the effective load, while when the isolated system steady state response is highly ultrasensitive (**C**), the bandwidth increases for small amounts of effective load if the input amplitude is sufficiently small. Large input amplitudes always result in decreased bandwidth with the addition of effective load.

Figure 2. Experimental system. A,B. *System with double load*: **A** shows the abstracted view (identities with the species of Fig. 1A are apparent) and **B** shows the detailed view of the UTase/UR-PII monocycle employing wild-type PII trimers. The sequential modification of the three subunits of the PII trimer are depicted along with the complexes that are bound by NRII. Light blue circles signify the uridylyl groups that modify each subunit. A modified subunit cannot bind NRII. Therefore, in the abstracted version of this system (panel A), PII-UMP comprises the P_1, P_2, and P_3 species as each of these has at least one modified subunit. **C,D**. *System with single load:* **C** shows the abstracted view (comparing to Fig. 1A, we have $\alpha=0$) and **D** shows the detailed view of the UTase/UR-PII monocycle employing heterotrimeric, "monovalent", PII. The monovalent PII is depicted as containing two mutant subunits (black) and one wild-type subunit that can be reversibly modified or bind to NRII.

Figure 3. SIM increases the response time in the zero-order regime and decreases it in the first-order regime. A. Rise time of wild-type system. All samples lacked glutamine, and the uridylylation process was initiated by addition of nucleotides. Black line, isolated system; red line, connected system (+ NRII). Reaction conditions were: 3 μM PII, 0.025 μM UTase/UR, 0.2 mM α-ketoglutarate, 1 mM α-[^{32}P]-UTP, 1 mM ATP, 0.3 mg/mL BSA, +/- NRII 10 μM. Reaction was at 30 ^{o}C. The PII modification was measured as previously [20]. The response time of the isolated system (no NRII) is indicated by the black arrow, while the response time of the connected system (with NRII) is indicated by a red arrow. **B**. Decay time for the wild-type system. After allowing the complete uridylylation of PII in the absence of glutamine, a saturating concentration of glutamine (10 mM) was added at 10 min (arrow). Conditions were as in Panel A, except that UTase/UR was 1.5 μM. **C**. Rise time of the system containing monovalent PII. Reaction conditions were as in Panel A except that heterotrimeric PII formed

from a 1:6 ratio of wild-type to PII-Δ47-53 subunits was used, at a concentration of 2 μM wild-type subunits, and UTase/UR was 0.012 μM. Reaction was at 30 ^{o}C. **D**. Decay time of system containing monovalent PII. Conditions were as in Panel C, except that UTase/UR was 0.5 μM and glutamine was added to 10 mM at 10 min. **E**. Decay time of system with wild-type PII and 0.8 mM glutamine (non-saturating concentration) added at 10 min.

Figure 4. SIM decreases system bandwidth. A, B and **C.** Performance of the UTase/UR-PII monocycle with periodic input stimulation of increasing frequency. The reaction mixtures contained 3 μM PII, 1.5 μM UTase, glutaminase consisting of 75 μM PLPS (24-mer) and additional 15 μM PdxT (to ensure saturation of the PLPS with the T subunits), and 10 μM NRII (red curves and points □) , or with no NRII (black curves and points ○). At indicated times (shown by the arrows), glutamine was added to 5 mM. For panel A, glutamine was added at 20 min and 60 min; for B, at 20 min, 45 min and 70 min; for C, at 20 min, 42 min and 64 min. **D**. Re-plot of the amplitude as a function of the frequency ω of the input stimulation from Panels A, B and C. The bandwidths for the isolated system ω_B^{I} and for the connected system ω_B^{C} are indicated by the arrows. For every frequency, the amplitude was calculated by taking the average of the excursions from each trough to each peak, starting from the first trough. **E, F** and **G**. UTase/UR-PII monocycle using monovalent PII as the substrate. The monovalent PII was formed from a 6:1 ratio of mutant to wild-type subunits, and was used at a concentration of 2 μM wild-type subunits. The reaction conditions were the same as in Panels A, B and C, except UTase was 1 μM. For E, glutamine was added at 30 min and 70 min; For F, at 30 min, 52 min and 74 min; For G, at 30 min, 50 min and 70 min. (H) Re-plot of the amplitudes as a function of the frequency of the input from Panels E, F and G.

Figure 5. The effect of the input amplitude on system bandwidth. UTase/UR-PII wild-type monocycle response to periodic input stimulation with increasing frequency for isolated (black curves and points ○) and connected (red curves and points □) system with 10μM NRII. **A, B** and **C.** The reaction conditions were the same as in Fig 4A, except that PLPS was 50 μM, and glutamine was added to 1.5 mM at indicated time points (as shown by the arrows). For A, glutamine was added at 10 min, 40 min and 70 min; for B, glutamine was added at 10 min, 28 min and 46 min; for C, glutamine was added at 10 min, 22 min and 34 min. **D.** Re-plot of amplitude as a function of the frequency of the input from Panels A, B and C.

Figure 6. Changing the enzyme amount impacts SIM. A, B and **C**. UTase/UR-PII wild-type monocycle under periodic input stimulation with decreasing UTase amounts, with 10 μM NRII (□ red points and curves) or with no NRII (○ black points and curves). The reaction conditions were the same as in Fig 4A, except that the UTase amount was varied. For A, UTase was 0.3 μM; for B, UTase was 0.1 μM; for C, UTase was 0.03 μM. **D.** Re-plot of amplitude as a function of UTase amounts from Panels A, B and C, and from Fig 4A. **E, F** and **G**. UTase/UR-PII monocycle with monovalent PII. The reaction conditions were the same as that of Fig 4E, except that the UTase amount was varied. For E, UTase was 0.1 μM; for F, UTase was 0.02 μM. G. Re-plot of amplitude as a function of UTase amounts from Panels E and F, and from Fig 4E.

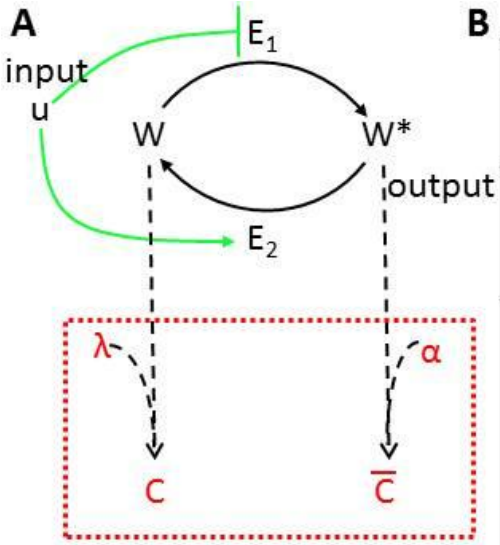

B

	Bandwidth	Relative Error $\Delta = 1 - \frac{A^C(\omega)}{A^I(\omega)}$
Double Load Ultrasensitive Regime $K_1.K_2 \ll W_T$	$\omega_B^C < \omega_B^I$ for large α, λ	$\frac{d\Delta}{dV} > 0$
Double Load Hyperbolic Regime $K_1.K_2 \gg W_T$ or Single Load (α=0) $K_2 \ll W_0,\ W_T - W_0 < K_1$	$\omega_B^C < \omega_B^I$	$\frac{d\Delta}{dV} < 0$

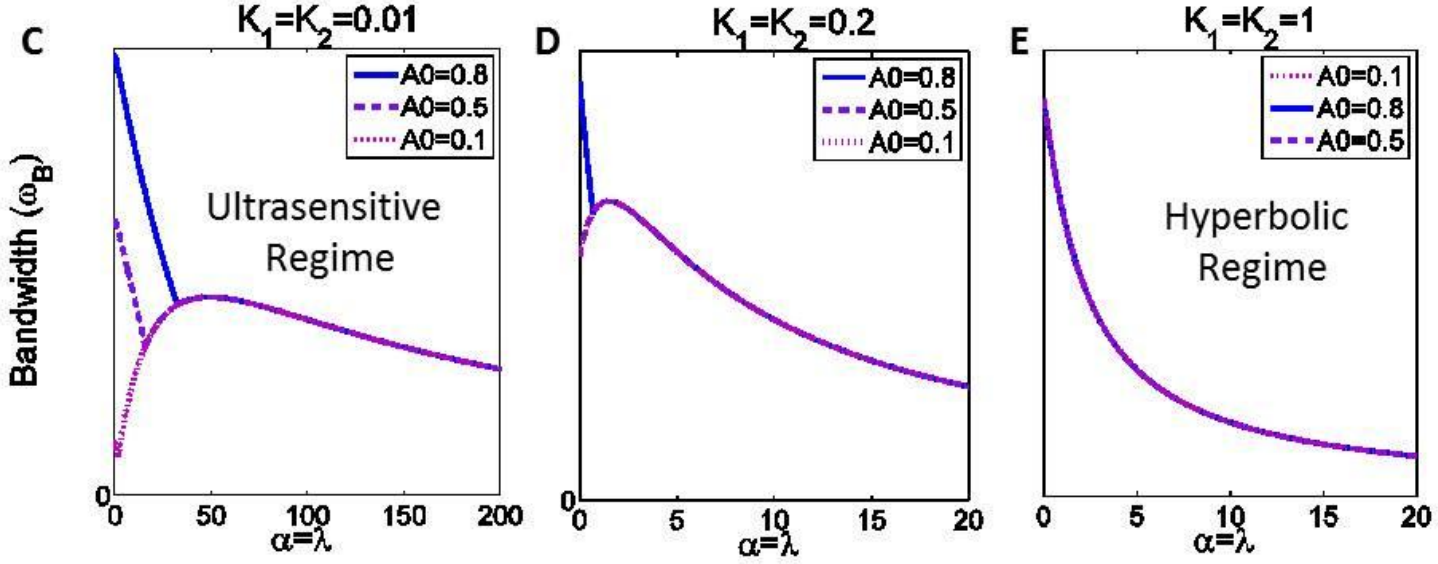

Fig 1

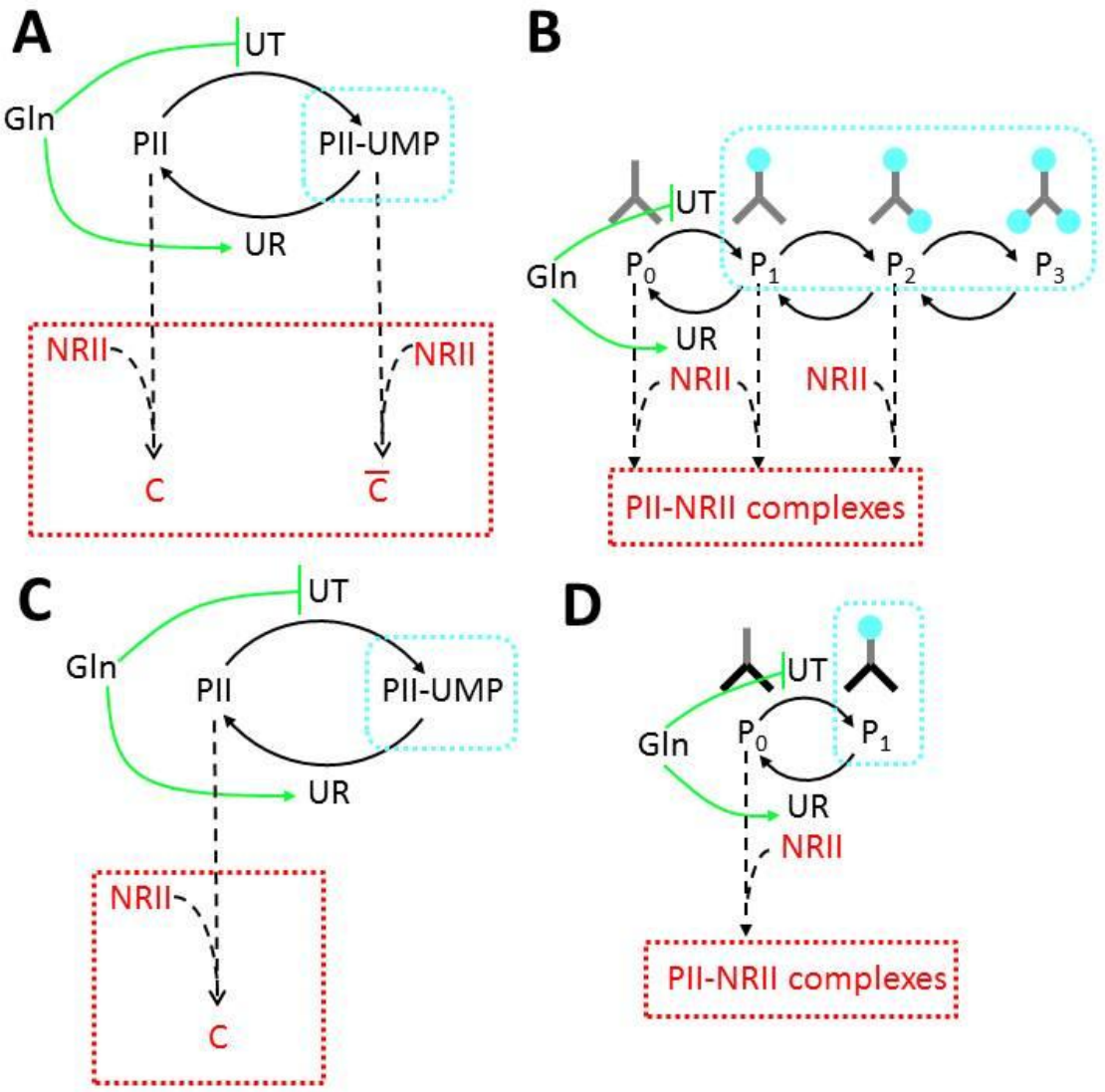
A
UT
Gln
PII
PII-UMP
UR
NRII
NRII
C
C
B
UT
Gln
P0
P1
P2
P3
UR
NRII
NRII
PII-NRII complexes
C
UT
Gln
PII
PII-UMP
UR
NRII
C
D
UT
Gln
P0
P1
UR
NRII
PII-NRII complexes

Fig 2

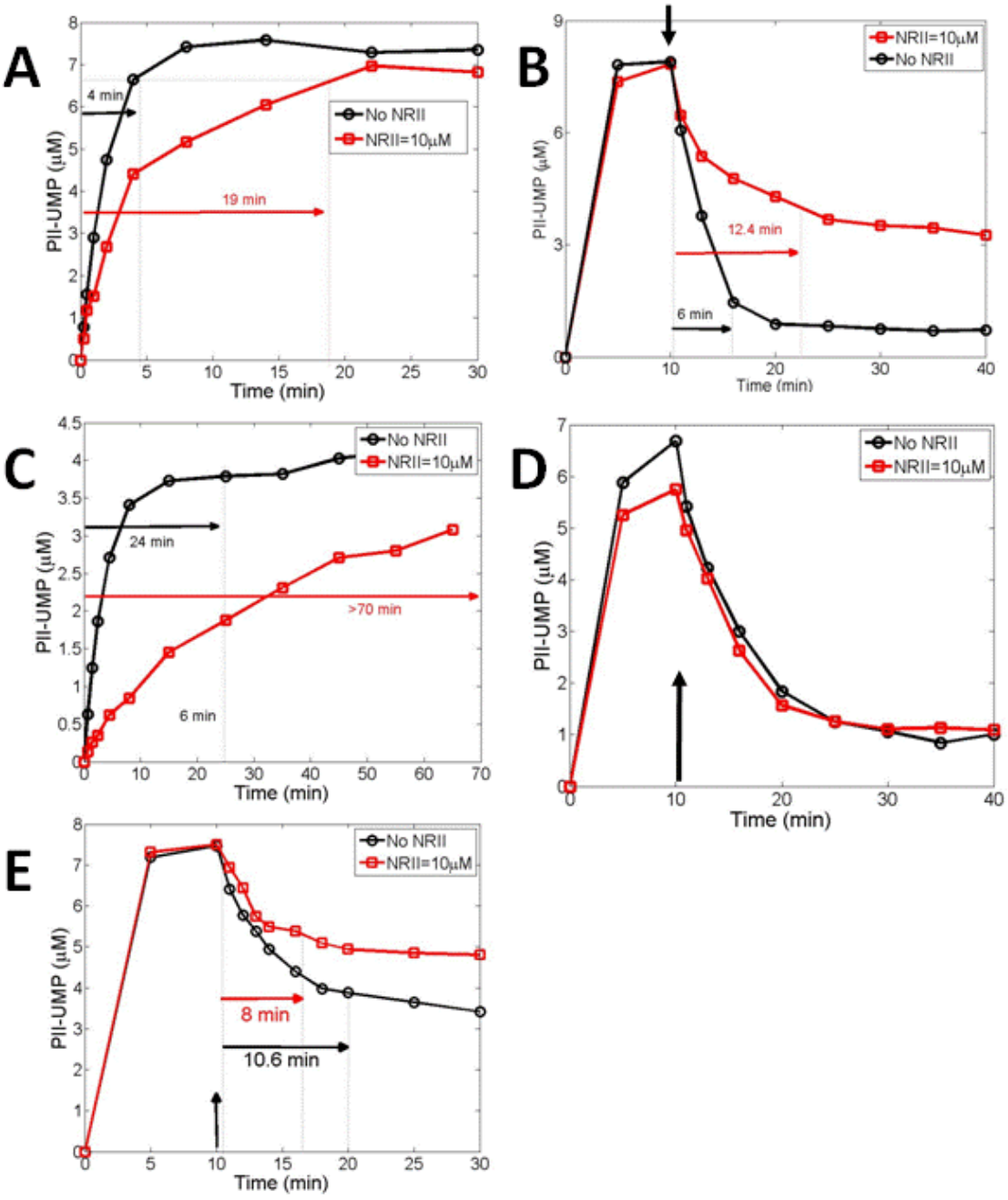
A
4 min
19 min
No NRII
NRII=10μM
PII-UMP (μM)
Time (min)
B
NRII=10μM
No NRII
12.4 min
6 min
PII-UMP (μM)
Time (min)
C
No NRII
NRII=10μM
24 min
>70 min
6 min
PII-UMP (μM)
Time (min)
D
No NRII
NRII=10μM
PII-UMP (μM)
Time (min)
E
No NRII
NRII=10μM
8 min
10.6 min
PII-UMP (μM)
Time (min)

Fig 3

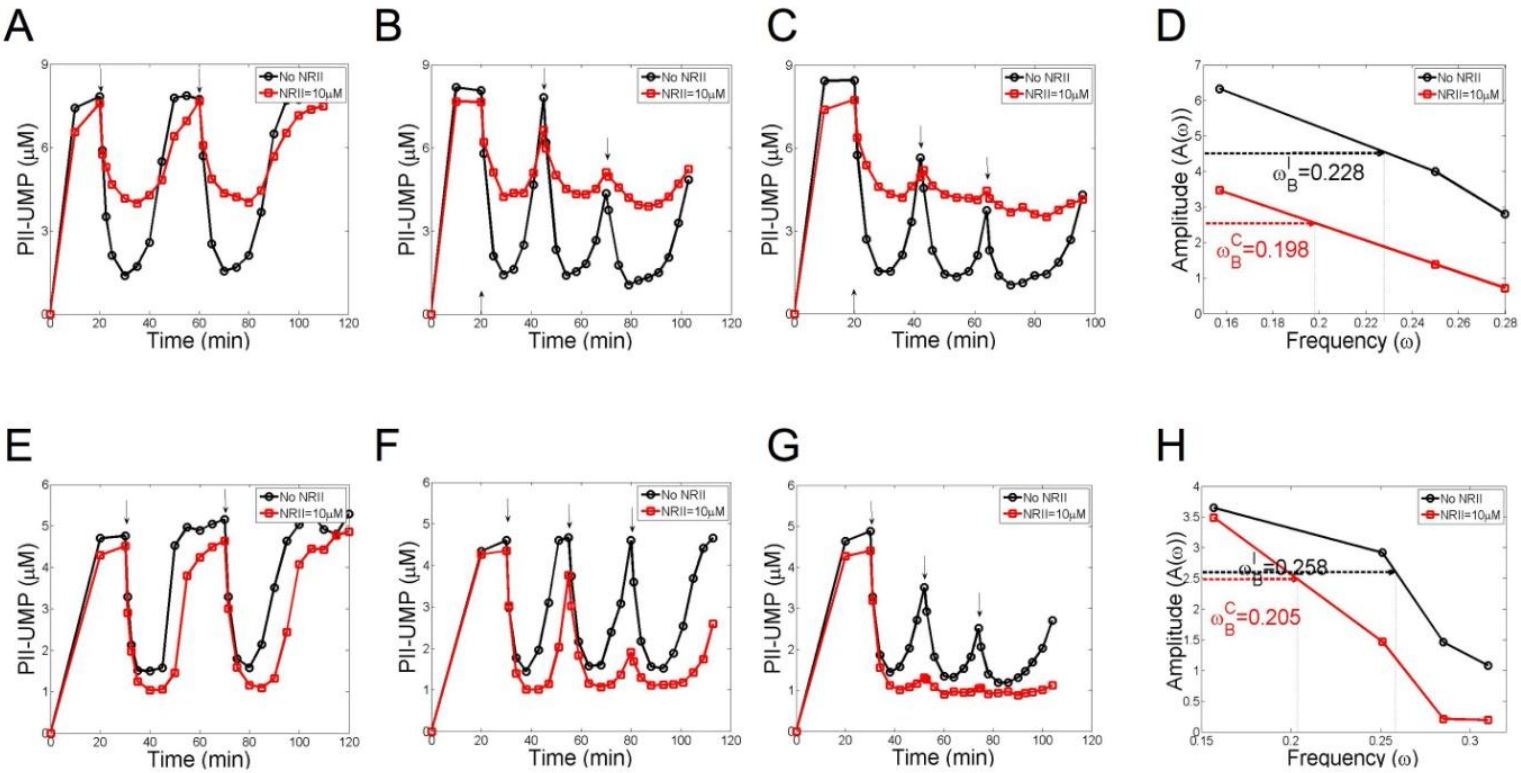
A
B
C
D
E
F
G
H
No NRII
NRII=10μM
PII-UMP (μM)
Time (min)
Amplitude (A(ω))
Frequency (ω)
ω_B^I=0.228
ω_B^C=0.198
ω_B^I=0.258
ω_B^C=0.205

Fig 4

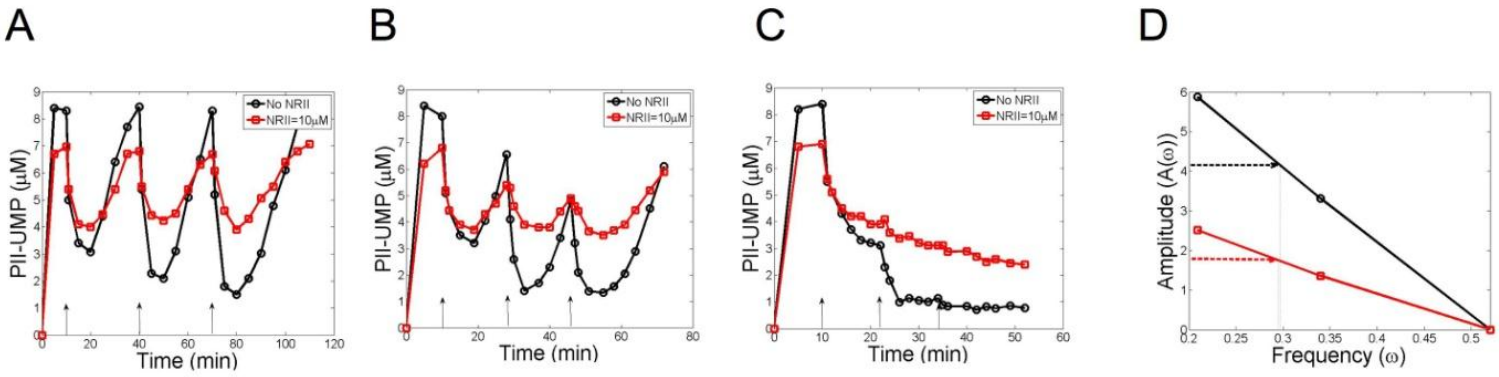
A
B
C
D
No NRII
NRII=10μM
PII-UMP (μM)
Time (min)
Amplitude (A(ω))
Frequency (ω)

Fig 5

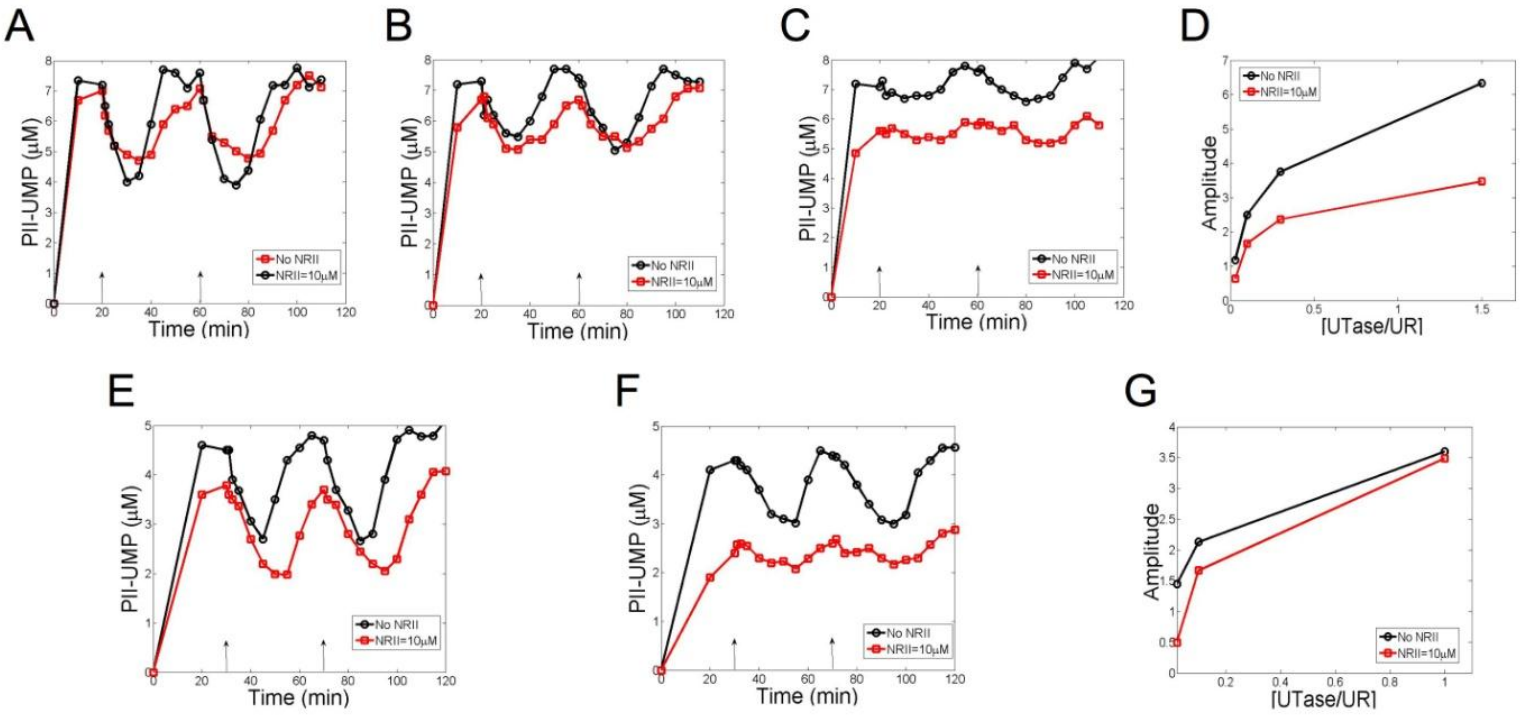
A
B
C
D
E
F
G
PII-UMP (μM)
Time (min)
No NRII
NRII=10μM
Amplitude
[UTase/UR]

Fig 6